


Microscale Isoelectric Fractionation Using Photopolymerized Membranes

Greg J. Sommer,* Junyu Mai, Anup K. Singh, and Anson V. Hatch

Biotechnology and Bioengineering Department, Sandia National Laboratories, Livermore, California 94550, United States

 Supporting Information

ABSTRACT: In this work, we introduce microscale isoelectric fractionation (μ IF) for isolation and enrichment of molecular species at any desired location in a microfluidic chip. Narrow pH-specific polyacrylamide membranes are photopatterned in situ for customizable device fabrication; multiple membranes of precise pH are easily incorporated throughout existing channel layouts. Samples are electrophoretically driven across the membranes such that charged species, for example, proteins and peptides, are rapidly discretized into fractions based on their isoelectric points (pI) without the use of carrier ampholytes. This format makes fractions easy to compartmentalize and access for integrated preparative or analytical operations on-chip. We present and discuss the key design considerations and trade-offs associated with proper system operation and optimal run conditions. Efficient and reproducible fractionation of model fluorescent pI markers and proteins is achieved using single membrane fractionators at pH 6.5 and 5.3 from both buffer and *Escherichia coli* cell lysate sample conditions. Effective fractionation is also shown using a serial 3-membrane fractionator tailored for isolating analytes-of-interest from high abundance components of serum. We further demonstrate that proteins focused in pH specific bins can be rapidly and efficiently transferred to another location in the same chip without unwanted dilution or dispersive effects. μ IF provides a rapid and versatile option for integrated sample prep or multidimensional analysis, and addresses the glaring proteomic need to isolate trace analytes from high-abundance species in minute volumes of complex samples.

A prevailing challenge in the proteomics and diagnostics communities involves detection and analysis of trace analytes from small volumes of complex samples, including clinical samples and rare cells. Techniques that exploit the pH-dependent electromobility of analytes (i.e., isoelectric focusing and fractionation) are widely used in macroscale preparative and analytical protocols, usually on the front-end of multidimensional separations or mass spectrometry.¹ However, when targeting low-abundance species these conventional methods suffer several major drawbacks including large sample volume requirements (several microliters), extensive sample dilution (often >100-fold), and long run times (several hours to days). A microscale approach may address these shortcomings and provide a complementary component in proteomic analysis workflows, particularly for small volume, precious samples.

Although extensive effort in the microfluidics arena has focused on implementing IEF methodology into an on-chip format,^{2–6} substantial limitations of the reported approaches indicate that simply scaling conventional IEF to on-chip platforms does not satisfy the present proteomic need. The bulk of these on-chip techniques are carrier ampholyte solution-based systems, making multidimensional manipulation of focused product difficult. Issues arise with resolution losses in dimensional transfer; dispersion is problematic at the microscale when attempting to further manipulate resolved species for multidimensional preparation or analysis steps.^{2,3} Ampholyte-based systems can be further challenged by temporal instability of the pH gradient, ampholyte interference with subsequent separations, and rapid ampholyte accumulation from buffer reservoirs into much smaller microchannel volumes. Advantages are gained

by using immobilized pH gradients (IPGs) that stabilize against flow;^{7,8} however, second dimensional transfer in these continuous gradient systems must occur by electrophoretic methods, which are impacted by dispersion exacerbated by inefficient transfer from initial state of electroneutrality. In this work, we explore microscale immobilized pH-specific membranes as a completely new and versatile approach for integrating isoelectric separations on-chip, where focused species can be effectively compartmentalized, enriched, and subsequently accessed by electrokinetics, pressure, or other means.

This approach, which we term microscale isoelectric fractionation (μ IF), draws on our capabilities in microscale membrane patterning^{9,10} and pH gradient immobilization⁷ and shares operational parallels with its macroscale counterparts.^{11–18} In proteomics and diagnostics, isoelectric fractionation is primarily used to isolate analytes-of-interest from other species present in a sample (such as serum or urine proteins) which can interfere with detection and identification using standard analytical techniques. Several commercial implementations employ pH-specific membranes fabricated with Immobilines, nonamphoteric buffering compounds that are chemically incorporated into the backbone of a polyacrylamide matrix upon polymerization. This chemistry enables precise control over fractionated pH values and eliminates the need for carrier ampholytes in the running buffer solution.

Received: January 10, 2011

Accepted: March 3, 2011

Published: March 18, 2011

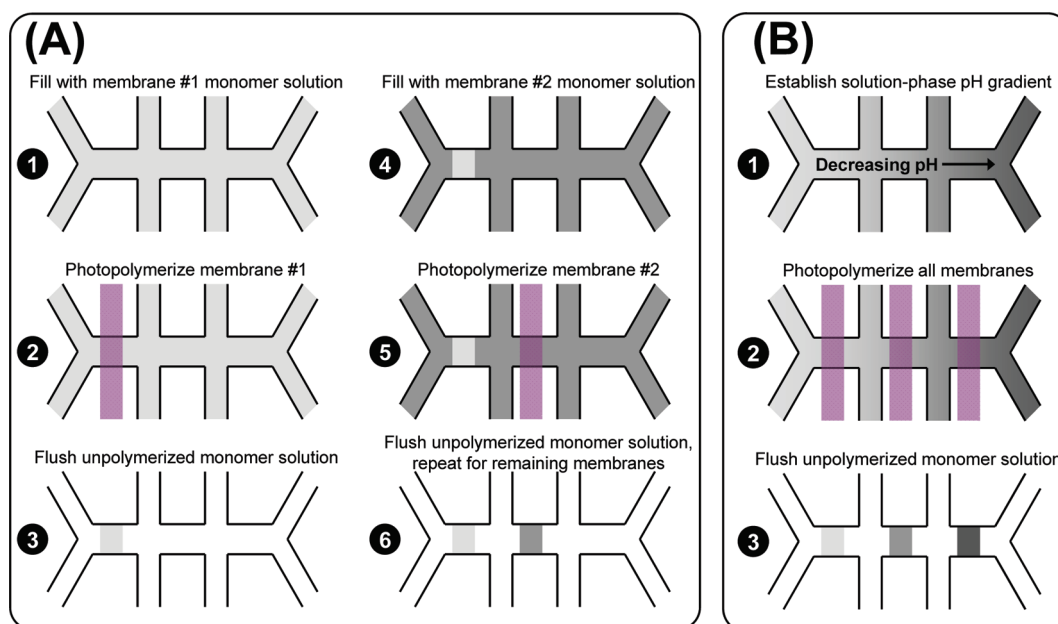


Figure 1. (A) Sequential photopolymerization of μ IF membranes. Aqueous monomer solutions are fed into channels via capillary action, and reservoirs are capped using a glass coverslip. Upon stagnation of all hydrodynamic flow in channels, the membrane region is exposed to a focused UV beam to photopolymerize the membrane. The unpolymerized solution is then flushed from the channels via vacuum, and the next monomer solution is loaded for polymerization. (B) Simultaneous photopolymerization of μ IF membranes. An aqueous pH gradient is first established along the μ IF channel axis according to protocols presented in ref 7. A photomask is then used to expose only the desired membrane regions to light from a UV lamp. Following polymerization, unpolymerized regions are flushed and rinsed twice with DI water and stored in buffer solution until use. Images not drawn to scale.

This work introduces μ IF methodology and demonstrates its utility in fractionating biological samples spiked with model protein analytes. We highlight key fabrication and operational parameters for optimizing device performance and present simple device architectures for single or multimembrane fractionation and subsequent transfer and integration with other on-chip processes, such as affinity depletion, digestion, hybridization, size-based separation, and immunoassays. Such integrated and automated platforms represent next-generation tools for molecular research and diagnostics technology.

MATERIALS AND METHODS

Reagents. Forty percent acrylamide solution, 3-(trimethoxysilyl)propyl methacrylate (98%), methylcellulose (MC), HEPES, Tris, lactic acid solution, mouse serum albumin (MSA), IgG from mouse serum (Ms-IgG), carbonic anhydrase isozyme II (CA), and bovine hemoglobin (Hb) were from Sigma (St. Louis, MO). 2,2'-Azobis[2-methyl-N-(2-hydroxyethyl)propionamide] photoinitiator (VA-086) was from Wako Chemicals (Richmond, VA). *N,N'*-Methylenebisacrylamide, Alexa Fluor 488-labeling kits, and low-MW fluorescent pI markers (pI 4.5, 5.5, 6.2, 6.8, and 7.2) were from Invitrogen (Carlsbad, CA); 0.2 M Immobiline solutions (pK 1, 3.1, 3.6, and 10.3) were from Fluka (Buchs, Switzerland). Human C-Reactive Protein (CRP) was from Lee Biosolutions (St. Louis, MO). 0.2 M Immobiline solutions (pK 4.6, 6.2, and 7.0), Cy2, Cy3, and Cy5 DIGE fluor labeling kits were from GE Healthcare (U.K.). MSA, Ms-IgG, CA, and CRP were labeled with CyDye and Alexa Fluor kits according to manufacturers' instructions. BL21 Star (DE3) *Escherichia coli* cells were purchased from Invitrogen, grown in Overnight Express TB Medium (Novagen, Madison, WI) for 6 h at 37 °C and 12 h at 22 °C. Following centrifugation, the cells were

harvested by 5000 g centrifugation for 5 min and resuspended in PBS. Cell lysate was captured by sonicating the cells and collecting the supernatant following centrifugation at 10 000 g for 10 min.

Device Fabrication. The fabrication and operational protocols reported here represent optimized procedures established through extensive testing and modification. The details of this iterative optimization are included in Supporting Information (SI).

Glass (fused silica) microdevices were designed in-house and fabricated at Caliper Life Sciences (Hopkinton, MA) using standard wet-etching techniques. Microchannels measured 100 μ m-wide \times 35 μ m-deep. 2 mm-diameter via holes were drilled into the top layer of the device to allow access to microchannels. An example device layout is shown in Figure 1(A). Channels were coated in-house with acrylate-terminated self-assembled monolayers via a 30 min incubation with a 2:3:5 (v/v/v) mixture of 3-(trimethoxysilyl)propyl methacrylate, glacial acetic acid, and deionized (DI) water. The channels were then rinsed twice with methanol, twice with DI water, thoroughly dried with a vacuum, and stored dry until membrane fabrication.

μ IF membranes were photopolymerized at precise locations within the microchannels using methods adapted from previous reports.^{7,9} The high surface-to-volume ratio of the microchannels allows the membranes to be secured in place solely by covalent binding to a silanized channel wall even with high voltage applied during electrophoresis, without using any supportive matrix or pillar structures. Our designs generally incorporated open fluid paths facilitating access to quickly remove unpolymerized monomer during fabrication and later fractionated sample components via flow. Membrane monomer solutions were mixed in 250 μ L volumes using recipes adapted from a commercial linear pH 3–7 IPG strip formulation.¹⁹ Further details regarding example

Table 1. Recipes for Fabricating pH 5.3 and 6.5 Membranes

| reagent | pH 5.3 | pH 6.5 |
|--------------------------|------------|------------|
| pK 1.0 Immobililine | 3.36 mM | 6.32 mM |
| pK 3.1 Immobililine | 13.4 mM | 10.2 mM |
| pK 3.6 Immobililine | 2.96 mM | 2.56 mM |
| pK 4.6 Immobililine | 3.36 mM | 2.56 mM |
| pK 6.2 Immobililine | 2.08 mM | 3.52 mM |
| pK 7.0 Immobililine | 5.36 mM | 5.44 mM |
| pK 10.3 Immobililine | 18.9 mM | 14.2 mM |
| acrylamide/bisacrylamide | 4%T, 10%C | 4%T, 10%C |
| VA-086 photoinitiator | 0.2% (w/v) | 0.2% (w/v) |
| Tris | 4 μ M | — |

recipes are shown in Table 1. Monomer solutions were mixed, vortexed, and pH tested using a benchtop pH meter. Solutions were then titrated to the desired pH with small volumes of the titrating acidic and basic pK Immobilines (pK 1.0 and 10.3). Monomer solutions with desired pH < 6.5 were titrated with small volumes of 1 M Tris to raise the solution to pH 6.5 for polymerization uniformity and efficiency purposes. Note that the Tris is subsequently removed by rinsing the polymerized gel and does not affect final membrane pH.

μ IF membrane fabrication can be achieved via two different methods, as shown in Figure 1A and B. In the first method, pH-specific monomer solutions are sequentially loaded into the entire device for piecemeal membrane photopolymerization. After loading the solution into the device, the via reservoirs are capped using a glass coverslip to prevent evaporation from the channels and hydrodynamic flow through the device. The device is placed upon an inverted epifluorescence microscope and untouched for >5 min to ensure hydrostatic equilibrium. Membranes are fabricated by focusing a 405 nm collimated LED source (Thorlabs, Newton, NJ) through a 20 \times objective into the desired region on the device for \sim 80 s. Note that z-position calibration is needed to produce membranes with reproducible and desired dimensions. The second method for fabricating μ IF membranes is shown in Figure 1B. Here, a monomeric pH gradient is first established across the center channel using the diffusion-induced gradient formation technique we previously presented.⁷ The pH gradient is maintained by ensuring a linear distribution of Immobililine species along the channel. However, instead of polymerizing an entire IPG, discrete membranes are polymerized by exposing the device to light from a UV exposure system through a custom photomask. Each membrane will have a precise and unique pH based on its position in the channel and the chosen boundary monomer solutions. In this way, multimembrane systems can be easily fabricated with just one UV exposure step, rather than using sequential loading/polymerization steps. Upon polymerization with either method, the unpolymerized monomer solution is removed from the device using a vacuum, and the channels are rinsed with DI water to remove any unpolymerized monomers from the membranes. Because performance and optimization strategies were evaluated for simple 1- up to 3-membrane systems, all results presented here were obtained using membranes fabricated using the first, sequential method of membrane photopolymerization.

The vacant channels are then coated with a linear 5% acrylamide solution to reduce EOF and protein adsorption to the side walls. This is accomplished by loading a solution of 5%

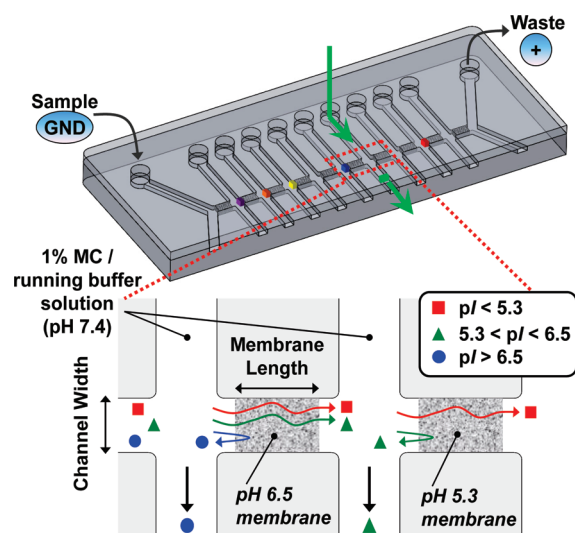


Figure 2. μ IF methodology. For illustrative purposes, the schematic depicts two membranes of pH 6.5 and 5.3 within a multimembrane fractionator (cross-section view). Charged species are loaded electrophoretically from a sample reservoir toward membranes of decreasing pH in the fractionation region. Samples with $pI < 6.5$ migrate through the pH 6.5 membrane, while $pI > 6.5$ samples are focused and extracted. Samples with $pI < 6.5$ continue to the second fractionation membrane, at which point samples with $pI < 5.3$ migrate through the pH 5.3 membrane, while $5.3 < pI < 6.5$ samples are isolated. Individual fractions can be transported via electrokinetics, pressure, or other means to adjacent channels for further processing and analysis.

acrylamide and 0.2% (w/v) VA-086 photoinitiator into the device, and exposing the entire microchip to a 500W (\sim 30W/cm²) flood UV lamp (OAI, San Jose, CA) for 360 s. The channels are then rinsed twice with DI water, and stored in a 5 mM HEPES, 2.4 mM Tris (pH 7.4) solution until use. Devices were usually tested within 0–2 days following fabrication.

Experimental Operation. The fundamental methodology behind μ IF is schematically shown in Figure 2. The isoelectric point (pI) denotes the pH at which a species' net charge is zero. A species will be positively charged at $pH < pI_{\text{species}}$ and negatively charged at $pH > pI_{\text{species}}$. The buffer pH determines electrophoretic transport toward or away from the membranes. In this system, experiments were constructed with buffer at pH 7.4 such that species with $pI < 7.4$ are electrophoretically driven toward the porous pH-specific membranes. Once they enter the membrane, they will either (a) continue through the membrane to the next region if they have $pI < pH_{\text{membrane}}$ or (b) stack at the membrane inlet boundary if they have $pI > pH_{\text{membrane}}$. In this manner, μ IF separates and concentrates species into discrete zones for preparation and analysis purposes.

For testing, the fractionator channels were loaded with a running buffer consisting of 5 mM HEPES, 2.4 mM Tris, and 1% (w/v) MC (pH 7.4). Buffer concentrations were considered high enough to maintain conductivity and electrophoretic transport of species between membranes but low enough so as not to exceed the buffer capacity of membranes. Devices were loaded into a custom manifold, as previously described,²⁰ allowing for \sim 60–120 μ L of running buffer or sample in each reservoir. The manifold was then mounted upon an inverted epifluorescence microscope for imaging using a 10 \times objective. Electric fields were applied through platinum electrode leads from a programmable high-voltage power supply designed and fabricated in-house.²⁰

Table 2. Optimized μ IF System Fabrication and Run Conditions Based on Extensive Testing (see SI for Experimental Details)

| design parameter | range tested | optimal condition | notes |
|--------------------------------|-----------------------------|------------------------|--|
| channel width | 100–500 μm | 100 μm | narrower channel increases membrane rigidity |
| membrane length | 50–300 μm | 200 μm | longer membranes enhance structural integrity and limit diffusive crossover, yet provide efficient transport of nonexcluded species |
| %T, %C of membrane | 3%T, 2.6%C to 10%T, 10%C | 4%T, 10%C | lower %T increases porosity, while higher %C increases rigidity |
| total Immobiline concentration | ~8–72 mM | ~48 mM | higher concentration improves buffering capacity, but is limited by immobilization efficiency |
| electric field strength | 20–360 V cm^{-1} | 120 V cm^{-1} | E-field must be high enough that electrophoresis overcomes diffusion through membrane, yet is limited by membrane integrity, concentration polarization, and joule heating |

For single-membrane fractionator testing, samples were first loaded into the sample (S) reservoir. Images were taken every 10 s during the run using a CoolSnap HQ interline CCD camera (Roper Scientific, Trenton, NJ) and Image-Pro Plus imaging software (MediaCybernetics, Bethesda, MD). Manual shuttering and a neutral density filter were used to reduce photobleaching. After 25 s without a field applied, the samples were driven across the membrane to a waste (W) reservoir under 120 V cm^{-1} for 60 s. The field was then switched to load from the clean buffer reservoir (B) across the membrane under the same field for 210 s. The field was then removed and images were taken for another 45 s. Three-membrane fractionator testing was accomplished in a similar manner by driving the sample and buffer across three membranes, rather than just one membrane. The sample load time was increased to 90 s, while the buffer wash remained 210 s for three-membrane testing. Electric field strengths of 120 V cm^{-1} were maintained for these runs. In all runs, a slight hydraulic head was placed on the reservoirs connected to the intersecting orthogonal channels to induce a slow flow through these channels; the purpose of this flow is to replace ions in the intermembrane region and reduce the effects of concentration polarization between the membranes.

Quantitative image analysis was accomplished using the same software to calculate the average fluorescent intensity in a small region-of-interest in front of the membrane inlet boundary. The data was normalized using the equation: $\text{ave} = ((\text{data} - \text{buffer}) / (\text{species} - \text{buffer}))$, where data is the average intensity at the membrane inlet boundary, buffer is the average intensity from the channel composed of only clean buffer, and species is the average intensity from the (unconcentrated) sample loading channel.

RESULTS AND DISCUSSION

Single-Membrane μ IF Characterization. To achieve superior fractionation performance, it is important to obtain optimal balance between the membranes' mechanical strength, pore size, and buffering capacity by adjusting key parameters of membrane composition and channel architecture. Detailed information regarding system characterization and optimization are included in SI, with a summary of the results shown in Table 2.

False-color, overlaid images of protein fractionation across individual membranes from intermittent time points are shown in Figure 3. Figure 3A shows the fractionation of hemoglobin (Hb, pI 6.8) and Cy3-labeled carbonic anhydrase (CA-Cy3, pI 5.9) across a pH 6.5 membrane. During the sample loading stage ($t = 80 \text{ s}$), both species initially accumulate at the membrane inlet

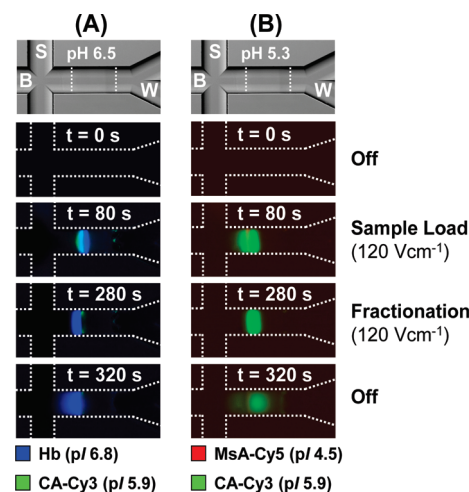


Figure 3. Characterization of single-membrane fractionators using fluorescently labeled proteins (false color, overlaid micrographs). Fractionation across (A) pH 6.5 membrane, and (B) pH 5.3 membrane. In both image sequences, all proteins stack at the membrane boundary during sample loading ($t = 80 \text{ s}$). Upon switching the E-field to fractionation using a clean buffer reservoir ($t = 280 \text{ s}$), the proteins are fractionated as those with $pI < pI_{\text{membrane}}$ migrate through the membrane (CA in (A) and MsA in (B)), while those with $pI > pI_{\text{membrane}}$ are focused (Hb in (A) and CA in (B)). Upon removal of the electric field, the stacked proteins diffuse away from the concentration zone ($t = 320 \text{ s}$). $E = 120 \text{ V cm}^{-1}$.

boundary. CA is passing through the membrane, but its mobility inside the membrane is slower than in the pH 7.4 liquid gel outside of the membrane, thereby causing accumulation. Upon switching the electric field to fractionation using a clean buffer reservoir ($t = 280 \text{ s}$), the Hb band remains stacked at the membrane inlet boundary, while the CA-Cy3 band passes entirely through the membrane as expected. Upon removal of the electric field ($t = 320 \text{ s}$), the Hb band diffuses away from the membrane inlet boundary, demonstrating that it is neither retained nor trapped in the membrane. Similar fractionation results are seen in Figure 3B for a different set of proteins: Cy5-labeled mouse serum albumin (MsA-Cy5, pI 4.5) and CA-Cy3, across a membrane with pH 5.3. At this lower membrane pH, the CA-Cy3 stacks at the membrane inlet boundary, while the MsA-Cy5 with even lower pI passes through as expected. Plots showing the concentration of each species stacking at the membrane inlet boundaries (measured by calculating the average

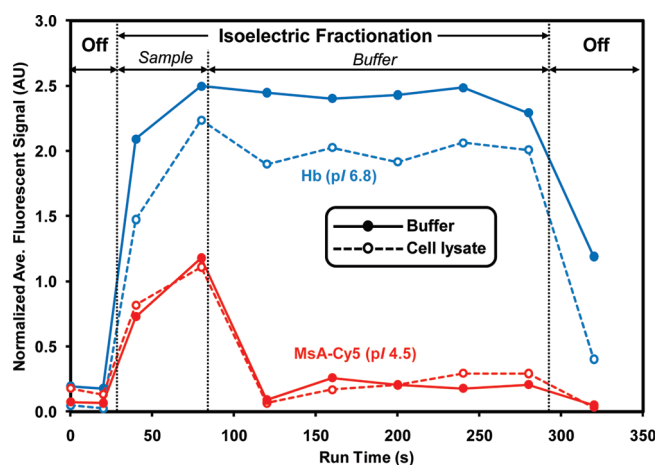


Figure 4. Concentration profiles of Hb and MsA-Cy5 spiked in both buffer and 20-fold diluted *E. coli* cell lysate, and separated across pH 6.5 fractionator using a 60 s sample injection and 210 s buffer fractionation. $E = 120 \text{ V cm}^{-1}$.

fluorescent intensity in a small region-of-interest in front of each membrane) versus time are shown in Figure S1 in SI.

μ IF in Cell Lysate. To demonstrate the utility of μ IF in analyzing more complex biological samples, fractionations of two fluorescent species spiked in both buffer and a 20-fold diluted cell lysate were performed using a pH 6.5 membrane. The result is quantitatively plotted in Figure 4. Analysis of the average fluorescent intensity of the stacked proteins shows greater concentration of the higher *pI* species with nearly complete retention during the fractionation, while the lower *pI* species migrates through the fractionator and thus its intensity reverts to baseline levels. Comparison of buffer vs cell lysate conditions shows nearly identical performance despite the added sample complexity. The slight decrease in concentration factor for the Hb species in cell lysate can be attributed to an increase in current through the device because of added background salts, and thus reduced mobility of the protein. Sample dilution helps maintain adequate membrane buffering capacity and species electromobility. Trace analyte dilution is overcome by membrane enrichment; Figures 4 and S1 show that 5–25 fold (depending on species mobility) concentration factors were achieved in just 60 s. Longer run times may be used for applications in which greater enrichment is required. The modular architecture of this fractionation system also facilitates integration other on-chip sample enrichment techniques including a size-exclusion membrane as presented here; we have previously demonstrated 3–4 order of magnitude enrichment factors in addition to options for rapid mixing and reactions using similar membrane and gel-based systems.^{9,21}

Multimembrane Fractionation. Fractionators were also fabricated with capacity for three serially arranged membranes. A brightfield image of this device is shown in Figure 5A. The first (far left) membrane in this device was fabricated with an uncharged 4%T, 10%C monomer mixture (no Immobilines). The second and third membranes were fabricated at pH 6.5 and pH 5.3, respectively, using the recipes from Table 1. The uncharged membrane in this system served as a prefilter as well as control to assess species transport through a membrane having no immobilized charge.

Figures 5B and C show false color, overlaid micrographs of fluorescent *pI* markers and proteins fractionated using this

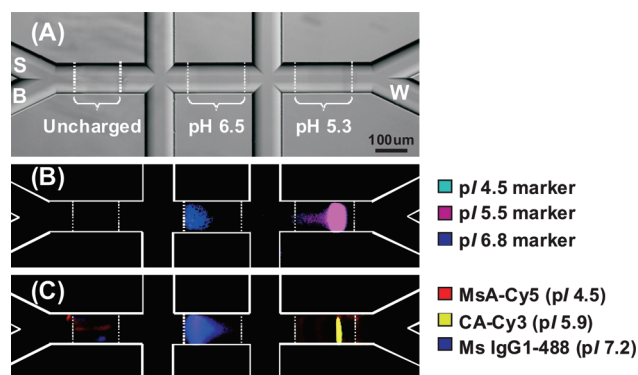


Figure 5. Three-membrane μ IF. (A) Brightfield image showing the locations of an uncharged 4%T, 10%C membrane, a pH 6.5 membrane, and a pH 5.3 membrane. Samples are loaded from the S reservoir for 90 s, followed by a buffer wash for 210 s, both under 120 V cm^{-1} . (B)-(C) False color, overlaid micrographs of (B) fluorescent *pI* markers, and (C) fluorescently labeled proteins shown following the fractionation step ($t = 280\text{s}$) with the E-field still applied.

device. Each marker and protein species either traverses or stacks at the appropriate membranes according to respective *pI* and pH. No species are retained in front of the uncharged 4%T, 10%C membrane, verifying that this polymer formula does not provide sized-based exclusion for these proteins of interest. A small quantity of MsA-Cy5 appears to have fouled each of the three membranes while loading, which is not surprising given MsA's strong tendency toward nonspecific adsorption. We also observed some undesirable stacking behavior that was not present in the single-membrane system. The species that are stacked at the pH 6.5 membrane (*pI* 6.8 marker and Ms-IgG1) have much broader, more diffusive bands than on single-membrane systems. When investigated, the bandwidth was relatively independent of the applied electric field strength. Meanwhile, the species that stack at the pH 5.3 membrane (*pI* 5.5 marker and CA-Cy3) tend to stack near the middle of the membrane, rather than at the inlet boundary. We believe that concentration polarization contributes to both of these stacking effects. A detailed hypothesis for this behavior is included in SI, and current efforts in our laboratory focus on improving the performance of multimembrane systems. Despite the difference between the three-membrane system and the single-membrane device, this initial demonstration highlights the power of μ IF for fast protein isolation and concentration in proteomic and diagnostic applications. Here we have isolated a *pI* fraction which represents only species in the sample in the range of $5.3 < pI < 6.5$. Species excluded from this fraction include IgG and albumin, which together account for >70% of the total protein content in serum.

Transfer of Isolated Fractions. Addressing the most problematic issue surrounding microfluidic IEF adoption, μ IF allows for facile capture and transfer of isolated fractions for further analysis within the microfluidic architecture. Figure 6 and the video in SI demonstrates compartmentalization of human CRP (*pI* 6.7) at a pH 6.0 μ IF membrane in the first dimension, followed by electrophoretic transfer to a nanoporous preconcentration membrane in a separate region of the chip. As we have previously shown,^{9,10,22} nanoporous membranes enable myriad preparative and analytical functions, including buffer exchange, mixing, sizing, and immunoaffinity-based detection. Analysis of the focused band's fluorescent signal reveals no detectable loss of the CRP during transfer.

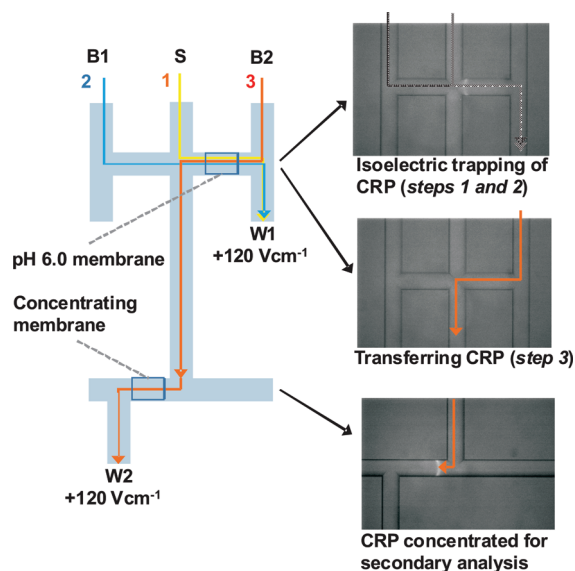


Figure 6. Transfer of isolated and enriched fraction to secondary analysis region. Using the microchannel geometry sketched in the schematic, human CRP-Cy2 (0.5 $\mu\text{g/mL}$, pI 6.7) is first stacked at the pH 6.0 μIF membrane in steps 1 and 2, then electrophoretically transferred to a nanoporous preconcentration membrane in a separate region of the chip.

This result illustrates the significant advantage of using discrete pH fractionation membranes as species electromobility is maintained despite reaching a location of electroneutrality because of the high pH buffer running between the membranes.

CONCLUSION

Here we have shown for the first time on-chip isoelectric fractionation using pH-specific membranes, a significant step toward integrated separation and detection of trace analytes from complex samples. The modular design of this novel electrophoretic system enables straightforward implementation with other on-chip proteomic preparatory and analysis techniques. For instance, μIF can be incorporated on the front-end of most on-chip immunoassays as a means to remove interfering proteins and other sample components prior to detection of a trace analyte. The resolution demonstrated here is adequate for many preparative applications, however improved resolution is only limited by the pH of each membrane and may be tuned using well-established Immobililine formulations used extensively in IPG strips.¹⁹ The capability to transfer focused species for subsequent analysis, combined with the selective and scalable fabrication approach, facilitates serial incorporation of μIF with on-chip processes, including lysis, chemical or enzymatic processing, mixing and binding reactions, affinity extraction or depletion, dialysis, and various chromatographic or electrophoretic separation methods. The ability to efficiently process volumes down to the nanoliter scale coupled with facile integration and automation with on-chip processes may greatly enhance future proteomic discovery, verification and end diagnostic capabilities.

ASSOCIATED CONTENT

S Supporting Information. Additional material as described in the text. This material is available free of charge via the Internet at <http://pubs.acs.org>.

AUTHOR INFORMATION

Corresponding Author

*Address: PO Box 969 MS 9291 Livermore, CA 94550. Phone: 925-294-2692. E-mail: gsommer@sandia.gov.

ACKNOWLEDGMENT

The authors would like to thank R. Meagher and Y. Light for providing cell lysate samples. This work was funded by Sandia's Laboratory Directed Research and Development program and NIAID #U01A1075441. Sandia is a multiprogram laboratory operated by Sandia Corp., a Lockheed Martin Co., for the United States Department of Energy under Contract DE-AC0494AL85000.

REFERENCES

- (1) Righetti, P. G.; Castagna, A.; Antonioli, P.; Boschetti, E. *Electrophoresis* **2005**, *26*, 297.
- (2) Sommer, G. J.; Hatch, A. V. *Electrophoresis* **2009**, *30*, 742.
- (3) Chen, H.; Fan, Z. H. *Electrophoresis* **2009**, *30*, 758.
- (4) Tia, S.; Herr, A. E. *Lab Chip* **2009**, *9*, 2524.
- (5) Li, H.-Y.; Dauriac, V.; Thibert, V.; Senechal, H.; Peltre, G.; Zhang, X.-X.; Descroix, S. *Lab Chip* **2010**, *10*, 2597.
- (6) Ishibashi, R.; Kitamori, T.; Shimura, K. *Lab Chip* **2010**, *10*, 2628.
- (7) Sommer, G. J.; Singh, A. K.; Hatch, A. V. *Anal. Chem.* **2008**, *80*, 3327.
- (8) Liang, Y.; Cong, Y.; Liang, Z.; Zhang, L.; Zhang, Y. *Electrophoresis* **2009**, *30*, 4034.
- (9) Hatch, A. V.; Herr, A. E.; Throckmorton, D. J.; Brennan, J. S.; Singh, A. K. *Anal. Chem.* **2006**, *78*, 4976.
- (10) Herr, A. E.; Hatch, A. V.; Throckmorton, D. J.; Tran, H. M.; Brennan, J. S.; Giannobile, W. V.; Singh, A. K. *Proc. Natl. Acad. Sci. U.S.A.* **2007**, *104*, 5268.
- (11) Righetti, P. G.; Wenisch, E.; Jungbauer, A.; Katinger, H.; Faupel, M. J. *Chromatogr. A* **1990**, *500*, 681.
- (12) Tang, H.-Y.; Speicher, D. W. *Expert Rev. Proteomics* **2005**, *2*, 295.
- (13) Righetti, P. G.; Bossi, A.; Wenisch, E.; Orsini, G. J. *Chromatogr., B: Biomed. Sci. Appl.* **1997**, *699*, 105.
- (14) Bier, M. *Electrophoresis* **1998**, *19*, 1057.
- (15) Bier, M.; Egen, N. B.; Allgyer, T. T.; Twitty, G. E.; Mosher, R. A. In *Peptides: Structures and Biological Function*; Gross, E., Meiehofer, J., Eds.; Pierce Chemical Company: Rockford, IL, 1979, p 79.
- (16) Faupel, M.; Barzaghi, B.; Gelfi, C.; Righetti, P. G. *J. Biochem. Biophys. Methods* **1987**, *15*, 147.
- (17) Zuo, X.; Speicher, D. W. *Proteomics* **2002**, *2*, 58.
- (18) Shave, E.; Vigh, G. J. *Chromatogr., A* **2007**, *1155*, 237.
- (19) Righetti, P. G. *Immobilized pH Gradients: Theory and Methodology*; Elsevier: Amsterdam, 1990.
- (20) Renzi, R. F.; Stamps, J.; Horn, B. A.; Ferko, S.; VanderNoot, V. A.; West, J. A. A.; Crocker, R.; Wiedenman, B.; Yee, D.; Fruetel, J. A. *Anal. Chem.* **2005**, *77*, 435.
- (21) Sommer, G. J.; Singh, A. K.; Hatch, A. V. *Lab Chip* **2009**, *9*, 2729.
- (22) Meagher, R. J.; Liu, P.; Light, Y. K.; Patel, K. D.; Perroud, T. D.; Singh, A. K. In *Proceedings of MicroTAS 2010*, Groningen, The Netherlands; The Printing House Inc: Stoughton, WI, 2010; p 1640.